THE JOURNAL OF BIOLOGICAL CHEMISTRY VOL. 287, NO. 2, pp. 1520–1526, January 6, 2012

High Temperature Requirement Factor A1 (*HTRA1*) Gene Regulates Angiogenesis through Transforming Growth Factor-β Family Member Growth Differentiation Factor 6*

Received for publication, July 3, 2011, and in revised form, November 1, 2011 Published, JBC Papers in Press, November 2, 2011, DOI 10.1074/jbc.M111.275990

Li Zhang[‡§1], Siok Lam Lim[§1], Hongjun Du[§], Ming Zhang[‡], Igor Kozak[§], Gregory Hannum[¶], Xiaolei Wang[‖], Hong Ouyang[§], Guy Hughes[§], Ling Zhao[§], Xuemei Zhu[§], Clara Lee[§], Zhiguang Su[‡], Xinrong Zhou[§], Robert Shaw[§], Dongho Geum[§], Xinran Wei[‡§], Jin Zhu[‡§], Trey Ideker[¶], Chio Oka[**], Ningli Wang[‖], Zhenglin Yang[‡‡2], Peter X. Shaw[‡§3], and Kang Zhang[‡§4]

From the [‡]Molecular Medicine Research Center and Department of Ophthalmology, West China Hospital, Sichuan University, Chengdu 610041, China, the [§]Institute for Genomic Medicine and Shiley Eye Center and [¶]Department of Bioengineering, University of California at San Diego, La Jolla, California 92093, the [‖]Tong Ren Eye Hospital, Beijing, China, the [**]Division of Gene Function in Animals, Nara Institute of Science and Technology, 8916-5 Takayama, Ikoma, Nara 630-0192, Japan, and [‡‡]The Sichuan Provincial Key Laboratory for Human Disease Gene Study and The Institute of Laboratory Medicine, Sichuan Academy of Medical Sciences and Sichuan Provincial People's Hospital, Chengdu, Sichuan 610072, China

Background: Genetic variants of high temperature requirement factor A1 (HTRA1) associate with AMD risk.
Results: Growth differentiation factor 6 (*GDF6*) gene polymorphism significantly associated with AMD. HTRA1 knock-out mice display reduced blood vessel in retina and up-regulation of GDF6.
Conclusion: HTRA1 regulates angiogenesis via TGF-β signaling by *GDF6*, a novel disease gene.
Significance: This novel pathway of HTRA1 in regulation of vascularization is critical for understanding AMD pathogenesis.

Genome-wide association study (GWAS) has identified genetic variants in the promoter region of the high temperature requirement factor A1 (*HTRA1*) gene associated with age-related macular degeneration (AMD). As a secreted serine protease, HTRA1 has been reported to interact with members of the transforming growth factor-β (TGF-β) family and regulate their signaling pathways. Growth differentiation factor 6 (GDF6), a member of the TGF-β family, is involved in ectoderm patterning and eye development. Mutations in GDF6 have been associated with abnormal eye development that may result in microphthalmia and anophthalmia. In this report, we identified a single nucleotide polymorphism (SNP) rs6982567 A/G near the *GDF6* gene that is significantly associated with AMD (p value = 3.54×10^{-8}). We demonstrated that the GDF6 AMD risk allele (rs6982567 A) is associated with decreased expression of the *GDF6* and increased expression of *HTRA1*. Similarly, the HTRA1 AMD risk allele (rs10490924 T) is associated with decreased *GDF6* and increased *HTRA1* expression. We observed decreased vascular development in the retina and significant up-regulation of *GDF6* gene in the RPE layer, retinal and brain tissues in HTRA1 knock-out (*htra1*$^{-/-}$) mice as compared with the wild-type counterparts. Furthermore, we showed enhanced SMAD signaling in *htra1*$^{-/-}$ mice. Our data suggests a critical role of HTRA1 in the regulation of angiogenesis via TGF-β signaling and identified *GDF6* as a novel disease gene for AMD.

Age-related macular degeneration (AMD)[5] is the leading cause of blindness among elderly patients in developed countries (1). Advanced AMD can be categorized as geographic atrophy or choroidal neovascularization (CNV). Geographic atrophy, also called dry AMD, is characterized by regional retinal pigment epithelium (RPE) loss and the eventual degeneration of overlying photoreceptors. CNV, also known as wet AMD, is characterized by growth of blood vessels from the choroid through the Bruch membrane toward the retina. In the case of CNV, bleeding and fluid leakage often occur due to abnormal angiogenesis, resulting in acute loss of central vision. Although the pathogenesis of AMD is still largely unknown, it has been reported that abnormal vascular growth mediated by vascular endothelial growth factor or other angiogenic factors plays a pivotal role in the pathogenic angiogenesis process in CNV (2–4).

Our previous research has identified that HTRA1 on chromosome 10q26 influences the risk of AMD (5). HTRA1 may modulate AMD development through many potential pathways. Multiple substrates of HTRA1 have been identified,

* This work was supported, in whole or in part, by a National Institutes of Health grant from the NEI, National Basic Research Program of China Grant 973 Program, No. 2011CB510200, Chinese National 985 Project to Sichuan University and West China Hospital, a Veterans Affairs Merit Award, Research to Prevent Blindness, and a BWF Clinical Scientist Award in Translational Research (to K. Z.).
[1] Both authors contributed equally to this work.
[2] Supported by National Natural Science Foundation of China Grant 81025006. To whom correspondence may be addressed. E-mail: zliny@yahoo.com.
[3] To whom correspondence may be addressed. E-mail: pshaw@ucsd.edu.
[4] To whom correspondence may be addressed: 9500 Gilman Dr., La Jolla, CA 92093-0838. Tel.: 858-246-0823; Fax: 858-246-0961; E-mail: kang.zhang@gmail.com.

[5] The abbreviations used are: AMD, age-related macular degeneration; CNV, choroidal neovascularization; RPE, retinal pigment epithelium; CARASIL, cerebral autosomal recessive arteriopathy with subcortical infarcts and leukoencephalopathy; SNP, single nucleotide polymorphism; IPL, inner plexiform layer; GDF, growth differentiation factor; HTRA1, high temperature requirement factor A1.

including aggrecan, decorin, biglycan, fibromodulin, fibronectin, and transforming growth factor-β (TGF-β) family members (6, 7). One of the major functions of HTRA1 is its ability to repress signaling by members of the TGF-β family (8, 9). A recent study found that mutants of HTRA1 with diminished protease activity resulted in dysregulation of vascular growth of small blood vessel in the brain, causing cerebral autosomal recessive arteriopathy with subcortical infarcts and leukoencephalopathy (CARASIL, a nonhypertensive cerebral small-vessel arteriopathy) (10). The mutant HTRA1 proteins failed to suppress TGF-β activity, leading to increased expression of TGF-β1 in the tunica in affected small arteries. These findings indicate that CARASIL is a vascular disease associated with dysregulation of TGF-β signaling (10). As a secreted protein, HTRA1 binds to several members of the TGF-β family, such as TGFβ1, TGFβ2, activin, bone morphogenetic protein 4, and growth differentiation factor 5 (GDF5) (8). Interaction of HTRA1 with these factors alters the signaling pathways mediated by the binding of these factors with their receptors (11). GDF6 is a member of the TGF-β family and has been found to express in the dorsal retina of developing mouse, *Xenopus*, and zebrafish (12, 13). It has been proposed that GDF6 may regulate ectoderm patterning (13) and control eye development by regulating neural and vascular development (14, 15). GDF6 mutations have been associated with eye phenotypes such as microphthalmia and anophthalmia (14).

In this report, we performed a genetic association study and identified a single nucleotide polymorphism (SNP) rs6982567A/G near *GDF6* that is significantly associated with AMD. The risk allele in rs6982567 was found to associate with decreased levels of *GDF6* and increased levels of *HTRA1* gene expression. Similarly, the HTRA1 AMD risk allele is also associated with decreased *GDF6* and increased *HTRA1* expression. In the retina of HTRA1 knock-out (*htra1*$^{-/-}$) mice, we observed decreased vascular development as well as significant up-regulation of *gdf6* and down-regulation of *vegf* gene levels in the RPE layer in comparison to the wild-type mice. Furthermore, as downstream effectors of GDF6 signaling, increased levels of phosphorylated SMAD1/5/8 were detected in the brain tissue of *htra1*$^{-/-}$ mice, suggesting that loss of HTRA1 affects regulation of signaling pathways involving the TGF-β family members. Our data supports a critical role of HTRA1 in the regulation of angiogenesis via TGF-β signaling and identified *GDF6* as a novel disease gene for AMD.

EXPERIMENTAL PROCEDURES

Patients—This study was approved by the Institutional Review Boards of the West China Hospital and University of California, San Diego. Subjects gave informed consent prior to participation. Participants underwent a standard examination, which included visual acuity measurements, dilated slit lamp biomicroscopy, and stereoscopic color fundus photography. Grading was carried out with the classification established by Age-related Eye Disease Study (AREDS) (16). Diagnosis of advanced AMD was based on the presence of CNV (equivalent to AREDS category 4 or 5). Control subjects were defined as being >60 years old, having fewer than 5 small drusen (<63 μm), and no RPE abnormalities. 2313 unrelated Caucasian individuals of European descent comprising 1538 AMD patients and 775 normal controls from the San Diego area participated in this study. An independent cohort of 3307 unrelated Caucasian individuals comprising 2158 AMD patients and 1149 normal controls was drawn from the Michigan, Mayo, Age-related Eye Disease Study, Pennsylvania (MMAP) Cohort Study (National Eye Institute, accession number phs000182.v2.p1).

Genotyping—SNPs were genotyped by SNaPshot on an ABI 3130XL analyzer (ABI, Foster City, CA) as previously described (17). For rs6982567A/G, primers 5′-AAAGAGGTTCAGGGGATTTACA-3′ and 5′-GGGCAGCTCAAGTCCTAATG-3′ were used to generate the amplicon encompassing the SNP by standard PCR; 5′-GTTTGATCCTTTCATCTTGATTAGGTCTGAGAGAGATTTTTTCCACATGTAGTCCT-3′ was used as the SNaPshot primer. For rs10490924 T/G, primers 5′-GCAAGTCTGTCCTCCTCGGT-3′ and 5′-GTCTGGGGTAAGGCCTGATCAT-3′ were used to generate the amplicon encompassing the SNP by standard PCR. 5′-CAAACTGTCTTTATCACACTCCATGATCCCAGCT-3′ was used as the SNaPshot primer. Genotyping success rate was >98% and accuracy was >99% as judged by random re-sequencing of 20% of the samples in case-control series.

Animals—All animal experiments followed the guidelines of the Association for Research in Vision and Ophthalmology (ARVO) Statement for the Use of Animals in Ophthalmic and Vision Research and were approved by the Animal Care Committee of University of California, San Diego, and West China Hospital, Sichuan University. Homozygous *htra1*$^{-/-}$ mice were generated by standard gene targeting procedures as described previously (18). Briefly, positive ES cell clones were microinjected into C57BL/6J blastocysts to generate chimeras. Heterozygous *htra1*$^{+/-}$ mice were obtained by crossing chimeras with C57BL/6J mice. The homozygous *htra1*$^{-/-}$ mice were produced by inbreeding of the *htra1*$^{+/-}$ mice. For genotyping, the targeted mutant allele was identified by PCR with a forward primer (5′-AATGGGCTGACCGCTTCCTCGTGCTT-3′) and a reverse primer (5′-TGTGCACGCCGTCGTACTGT-3′). The wild-type allele was identified with a forward primer (5′-CACTACGCATTGCAGCCCCTC-3′) and a reverse primer (5′- CGTACCACGCTCCTGTCTTT-3′). Genotypes were confirmed by PCR of genomic DNA extracted from tail snips. Wild-type C57BL/6 littermate mice served as normal controls.

Histology of Retinal Vasculature—The animals were sacrificed and eyes were fixed with 4% paraformaldehyde in PBS at 4 °C for 2 h (adult) or overnight (7-day postnatal). After three washes with PBS, the eyes were then cut 1-mm behind the limbus, and the anterior segments including cornea, iris, and lens were removed under a microscope. After being separated from the sclera, the retina were placed on a glass slide with their inner surface facing upwards and flattened by making 4 radial cuts on the edge of the retina. The vitreous were gently removed from the retinal surface using forceps. The retina were subsequently incubated with 0.5% fluorescein isothiocyanate (FITC)-isolectin B4 (Vector Laboratories, Burlingame, CA) overnight. Blood vessels were visualized with blue argon laser wavelength (488 nm) using a scanning laser confocal microscope FV1000 (Olympus Corporation of the Americas, Center Valley, PA).

TABLE 1
Primer sets used for real-time quantitative PCR

Gene amplified	Forward sequence (5′ → 3′)	Reverse sequence (5′ → 3′)
hu GAPDH	GAGTCAACGGATTTGGTCGT	GACAAGCTTCCCGTTCTCAG
hu GDF6	TGCACGTGAACTTCAAGGAG	CCCGCGTCGATGTATAGAAT
hu HTRA1	GGCTAGTGGGTCTGGGTTTAT	ACCGTTCTTCAGCTCAACTTTG
mo gapdh	gtcaaggccgagaatgggaa	ttggctccacccttcaagtg
mo gdf6	tatcgcgcccctagagtacg	atgctaatgggagtcagtttgg
mo htra1	catctccttcgcaattccat	gacggtccttcagctctttg
mo vegf	ggtggacatcttccaggagt	tgatctgcatggtgatgttg

TABLE 2
Association between single nucleotide polymorphism (SNP) rs6982567 A/G and AMD in Discovery, MMAP-CEU, and combination cohorts
For the Discovery cohort, 2313 unrelated Caucasian individuals of European descent comprising 1538 AMD patients and 775 normal controls participated in this study in San Diego area. For the MMAP-CEU cohort, 3307 unrelated Caucasian individuals comprising 2158 AMD patients and 1149 normal controls were drawn from the Michigan, Mayo, AREDS, Pennsylvania (MMAP) study cohort.

Cohort	Risk allele	AMD	Control	Affected frequency	Control frequency	Affected HWE	Control HWE	χ^2	P (allelic)
Discovery	A	1538	775	0.213	0.183	0.452	0.807	5.744	0.017
MMAP-CEU	A	2158	1149	0.206	0.154	0.54	0.84	26.739	2.33E-07
Combined	A	3696	1924	0.209	0.166	0.98	0.964	30.387	3.54E-08

Pictures for different layers of the retinal vasculature, including nerve fiber layer, inner plexiform layer, and outer plexiform layer were taken at the same distance from the optic head in each quadrant.

Retinal Vessel Density Examinations—We compared histology images of retinal blood vessels from both wild-type and *htra1*$^{-/-}$ mice at 7 days and 1 month postnatal. The images of retinal sections in different histological layers were processed using Adobe Photoshop (Adobe Systems Inc., San Jose, CA). The images were cropped and converted to black and white images. Pixel threshold of the images were determined, and then a Gaussian blur under Filter function was used to eliminate background signal and capture images of retinal vasculature only. Layer subtraction function under Image-Calculation-Subtract was used to calculate blood vessel density. The values between the two mouse types were compared using a paired *t* test.

Immunohistochemistry of Mouse Retina—Eyes from wild-type mice were sectioned and stained with rabbit anti-GDF6 IgG (Sigma) followed by anti-rabbit IgG conjugated with horseradish peroxidase. The VectorStain Elite ABC substrate kit (Vector Laboratories) was used for color reaction. The sections were then counterstained with methyl green. Images were captured using an Axio Observer A1 microscope (Carl Zeiss MicroImaging, Thornwood, NY).

Real-time PCR for Gene Expression—Total RNA was extracted from mouse tissues or human lymphocytes using the RNeasy Mini Kit (Qiagen Inc., Valencia, CA), and converted to cDNA using the SuperScript III First Strand Synthesis System (Invitrogen). All quantitative PCR experiments were performed with Power SYBR Green qPCR Master Mix (Applied Biosystems, Foster City, CA) and analyzed with the 7500 Real-time PCR Detection System (Applied Biosystems, Foster City, CA). Primer sets used are listed in Table 1. Relative mRNA levels were calculated by normalizing results using *GAPDH*, and then compared with tissues from wild-type littermates or human lymphocytes of protective genotypes.

Immunoblotting—Brain tissues were harvested from wild-type and *htra1*$^{-/-}$ mice. Tissue lysate was prepared using RIPA lysis buffer with phosphatase inhibitors (Cell Signaling Technology, Danvers, MA). Total protein concentrations were determined by a BCA assay (Bio-Rad) and normalized. Protein samples were resolved by SDS-PAGE and then transferred onto PVDF membrane and probed using anti-SMAD1 and anti-phospho-SMAD1/5/8 (Cell Signaling Technology). Immunoblot signal was measured and analyzed using ImageJ (imagej.nih.gov/ij) (19). Ratios of phosphor-SMAD/SMAD were determined.

Statistical Analysis—The initial genetic association analysis was carried out by constructing 2×2 tables of the allele counts and 2×3 tables of the genotype counts for each SNP in all cases and controls. Subsequently, Pearson χ^2 statistics were calculated and *p* values were computed by comparing the χ^2 statistic to a χ^2 distribution with 1 or 2 degrees of freedom for the allelic and genotypic tests, respectively. SNPs yielding a *p* value with statistical significance were selected for further analysis. The difference in vascular density and quantitative PCR data were analyzed with a paired Student's *t* test.

RESULTS

GDF6 Is Associated with Risk of AMD—One of the HTRA1 functions is to regulate signaling by TGF-β family members such as bone morphogenetic proteins or GDFs (8, 9). We investigated genetic associations of TGF-β family members with AMD. We found a single significant association, SNP rs6982567 located in 8q22.1 near the *GDF6* gene. A total of 2313 unrelated Caucasian individuals of European descent were genotyped as the first discovery cohort, which included 1538 AMD patients and 775 normal controls. The results demonstrated that the SNP rs6982567 was associated with AMD with statistical significance (allelic *p* value of 0.017). This association was validated in an independent cohort of Caucasian of European descent drawn from MMAP (2158 AMD cases and 1149 controls). After combining the Discovery cohort with the MMAP cohort, SNP rs6982567 showed a highly significant association with AMD (allelic *p* value of 3.54×10^{-8}), with risk allele frequency being 20.9% in cases *versus* 16.6% in controls (Table 2).

Reciprocal Regulation of Gene Expression between GDF6 and HTRA1—Because HTRA1 has been reported to regulate the TGF-β family signaling pathway, we first examined gene

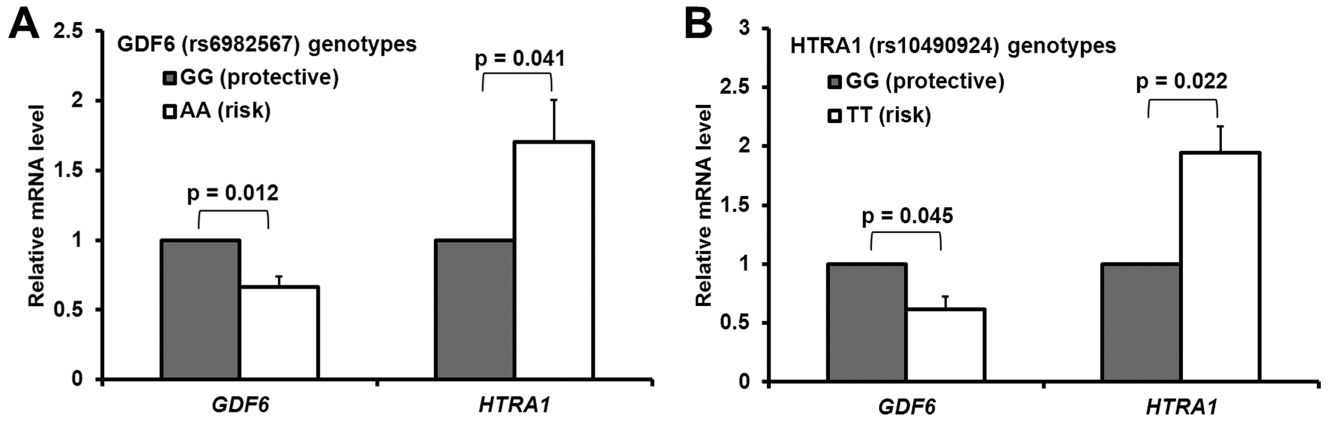

FIGURE 1. **Gene expression pattern of *GDF6* and *HTRA1* from human lymphocytes stratified by their (*A*) *GDF6* (rs6982567 A/G) or (*B*) *HTRA1* (rs10490924 T/G) genotypes.** Relative mRNA levels were calculated by normalizing with *GAPDH* and presented as relative levels to protective genotypes. *Error bars* represent S.E. For *GDF6* (rs6982567), $n = 5$ for GG genotype and $n = 4$ for AA genotype. For *HTRA1* (rs10490924), $n = 4$ for both GG and TT genotypes.

expression levels of *HTRA1* and *GDF6* in human lymphocytes stratified by their *GDF6* (rs6982567 A/G) genotypes using quantitative real-time PCR analysis. We found that for rs6982567, the *GDF6* mRNA level was 34% lower in lymphocyte samples of homozygous risk genotype AA than in the normal GG genotype ($p = 0.012$), whereas the *HTRA1* gene was up-regulated by 70% in the risk genotype ($p = 0.041$, Fig. 1*A*). Gene expression patterns of *GDF6* and *HTRA1* were also evaluated in human lymphocytes stratified by their *HTRA1* (rs10490924 T/G) genotypes. Similarly, the *GDF6* mRNA level was 38% lower in lymphocyte samples of homozygous risk TT genotype than in the normal GG genotype ($p = 0.045$), whereas *HTRA1* expression was up-regulated by 94% in the risk genotype ($p = 0.022$, Fig. 1*B*).

Reduction of Retinal Vasculature in htra1$^{-/-}$ Mice—Given that human patients with recessive HTRA1 mutations exhibited reduced cerebral small vessels and irregular vasculature in the brain (10), we reasoned that HTRA1 may play a similar role in the retinal vasculature. We compared 1-month-old *htra1*$^{-/-}$ mice ($n = 5$) with the same number of wild-type littermate controls (C57BL/6) for their retinal vessel density on three layers of retinal capillary beds. We observed reduced retinal capillary density on *htra1*$^{-/-}$ mice (Fig. 2*A*). The blood vessel densities for wild-type *versus htra1*$^{-/-}$ were 17.12 and 11.22 in nerve fiber layer ($p = 0.018$); 14.61 and 8.26 in the inner plexiform layer ($p = 0.047$); and 14.36 and 9.11 in outer plexiform layer ($p = 0.032$), respectively (Fig. 2*B*). The same procedures were performed on 7-day postnatal wild-type and *htra1*$^{-/-}$ mice ($n = 8$) to study early postnatal retinal vasculature. A lower retinal vessel density was also observed in *htra1*$^{-/-}$ mice ($p = 0.0011$, Fig. 2, *C* and *D*).

Expression of gdf6 and Other AMD-related Genes in Mouse—GDF6 protein was detected in the ganglion cell layer, inner plexiform layer, and RPE in wild-type mouse retina by immunohistochemistry (Fig. 3*A*). We further examined the *in vivo* gene expression of *gdf6* and *htra1* as well as *vegf* in RPE layer, retinal tissue, and brain tissue from wild-type and *htra1*$^{-/-}$ mice. We found that removal of the *htra1* gene in mice significantly up-regulated *gdf6* gene expression and down-regulated *vegf* gene expression in the RPE layer (Fig. 3*B*). The removal of the *htra1* gene also significantly up-regulated *gdf6* in mouse retinal tissue and brain tissue, but had less impact on *vegf* level in these tissues (Fig. 3, *C* and *D*).

Increased Phosphorylation Level of SMAD in htra1$^{-/-}$ *Mice*—SMAD proteins are important downstream effectors of TGF-β family signaling pathways. To determine the impact of loss of HTRA1 on TGF-β family signaling, we assayed phosphorylation of SMAD proteins using brain tissue lysate from wild-type and *htra1*$^{-/-}$ mice ($n = 6$). Comparing to wild-type, a higher level of phosphorylated SMAD1/5/8 (2.28-fold) was detected in samples from *htra1*$^{-/-}$ mice ($p = 0.0197$, Fig. 4).

DISCUSSION

Previously, genetic association studies had identified a HTRA1 polymorphism strongly associated with the risk of AMD, likely due to the elevated level of HTRA1 expression (17, 18, 20). However, the precise molecular mechanism by which HTRA1 causes AMD is still largely unknown. Increasing evidence suggests that HTRA1 functions in regulation of development, cell growth, differentiation, and apoptosis. Dysfunctions of HTRA1 may impact aging diseases such as arthritis (7) and neurodegenerative diseases (21). HTRA1 is a multidomain protein that can affect signaling by members of the TGF-β family, which is closely associated with vascular angiogenesis and remodeling. TGF-β family members may have different roles in regulation of vascular endothelial and smooth muscle cells, depending on cellular and extracellular environment (10, 22). As an example, mutations in three members of the TGF-β superfamily, including *bone morphogenetic protein 4*, *GDF3,* and *GDF6,* have been associated with microphthalmia and anophthalmia (23, 24). GDF6 is also reported to affect eye development (15). In this study, we analyzed a SNP (rs6982567) variant near *GDF6* in 2313 unrelated European Caucasian individuals comprising 1538 AMD patients and 775 normal controls, and demonstrated that SNP rs6982567 is significantly associated with AMD. The significant association of this SNP with AMD was further validated in an independent replication cohort from the MMAP study. When combining our cohort with the independent cohort, the overall association is highly significant ($p = 3.54 \times 10^{-8}$).

We observed reciprocal regulation patterns in *GDF6* and *HTRA1* gene expression stratified by *GDF6* (rs6982567 A/G) or

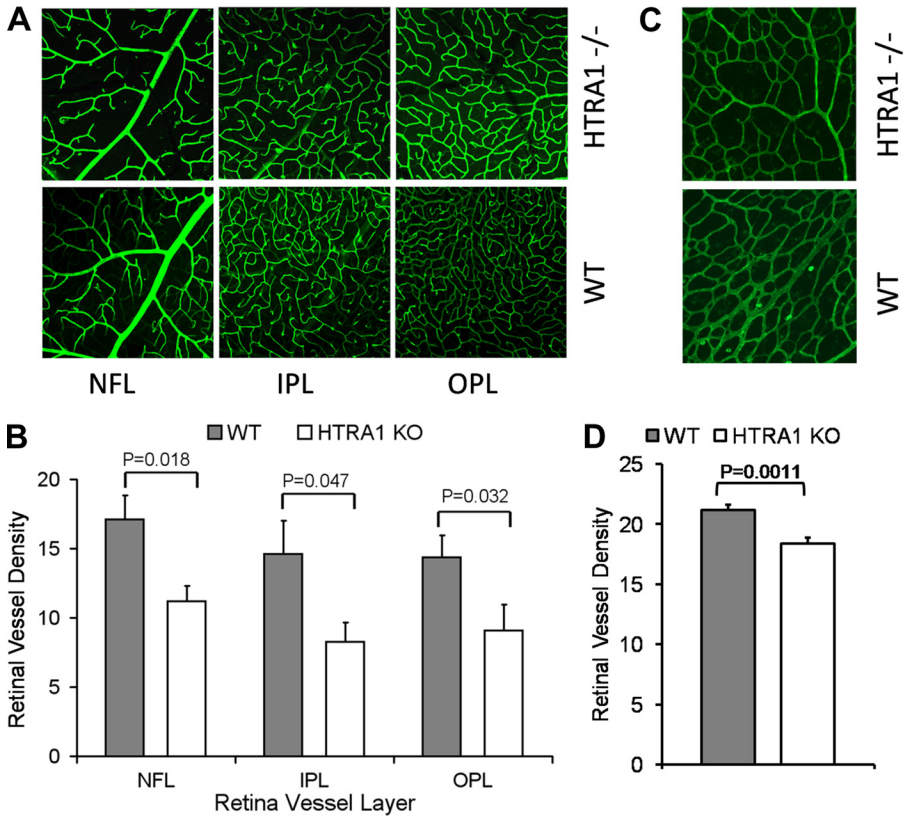

FIGURE 2. **Retinal vasculature development in mature and developing wild-type (C57BL/6) and *htra1*$^{-/-}$ mice.** *A,* histology images of retinal blood vessels in 1-month-old mice visualized by a scanning laser confocal microscope after FITC-isolectin staining. Pictures for different layers of blood vessel, including nerve fiber layer (*NFL*), inner plexiform layer (*IPL*), and outer plexiform layer (*OPL*) were taken at the same distance from the optic head in each quadrant. *B,* retinal vessel density in NFL, IPL and OPL from 1-month-old *htra1*$^{-/-}$ and wild-type mice. *C,* histology images of retinal blood vessels in 7-day-old mice visualized under a fluorescence microscope after FITC-isolectin staining. *D,* retinal vessel density in 7-day-old *htra1*$^{-/-}$ and wild-type mice. For 7-day-old mice, vessel density was examined for the whole retina due to the lack of defined vascular sublayers. Data were expressed as mean values. *Error bars* represent S.E. $n = 5$ for 1-month-old and $n = 8$ for 7-day-old mice.

HTRA1 (rs10490924 T/G) genotypes. In lymphocytes with a homozygous AMD risk genotype in either *GDF6* rs6982567 or *HTRA1* rs10490924, there was a down-regulation of *GDF6* expression with concomitant up-regulation of *HTRA1* expression. These findings suggest that as a member of the TGF-β family, GDF6 appears to be regulated by HTRA1 activity, and that dysregulation of a GDF6-related signaling pathway by HTRA1 likely contributes to AMD pathogenesis.

Because dysfunction of HTRA1 affects TGF-β family signaling in hereditary vascular disorders such as CARASIL, causing abnormal angiogenesis (10, 25), and our data also suggests that genetic polymorphisms resulting in up-regulation of *HTRA1* and down-regulation of *GDF6* are associated with risk of AMD, we investigated whether HTRA1 can affect vascular growth and impact *GDF6* expression *in vivo*. Our study showed that the vascular development in developing and mature *htra1*$^{-/-}$ mice is significantly attenuated compared with that in the wild-type littermates, indicating a crucial role of the HTRA1/GDF6 interplay in retinal vasculature development and maintenance.

In mouse eye, GDF6 expression was detected in the ganglion cell layer, IPL and RPE layers. We also showed that the *gdf6* level was up-regulated, whereas the *vegf* level was down-regulated in RPE from *htra1*$^{-/-}$ mice. These findings suggest that HTRA1 is an important factor regulating normal vascular growth during development, possibly via down-regulation of GDF6. This is consistent with a recent study showing that functional mutations of HTRA1 resulted in dysregulation of TGF-β signaling, resulting in a small blood vessel phenotype with ischemic cerebral disease and stroke in the brain. Mutations in the TGF-β signaling pathway have been reported to lead to hereditary hemorrhagic telangiectasia, Marfan syndrome, and associated vascular disorders (25–29). Our results further support a critical role of the TGF-β signaling pathway in vascular development and diseases.

A comprehensive study was previously carried out by Mazerbourg *et al.* (30) to identify the downstream signaling effectors corresponding to a spectrum of TGF/bone morphogenetic protein/GDF-related ligands using genomic analyses and *in vitro* assays. The authors demonstrated that GDF6 shares downstream signaling molecules with many other TGF-β ligands, and functions specifically through the SMAD1/5/8 pathway by induction of phosphorylation. It has also been reported that GDF6 knockdown resulted in reduced SMAD1/5/8 phosphorylation in *Xenopus* eye, specifically in the dorsal retina area (11). We observed significantly higher levels of SMAD1/5/8 phosphorylation in *htra1*$^{-/-}$ mice, suggesting that the loss of HTRA1 leads to up-regulated expression of GDF6 and enhanced activation of TGF-β signaling.

Ours and others' work suggest that an appropriate level of HTRA1 is required for vascular development and maintenance

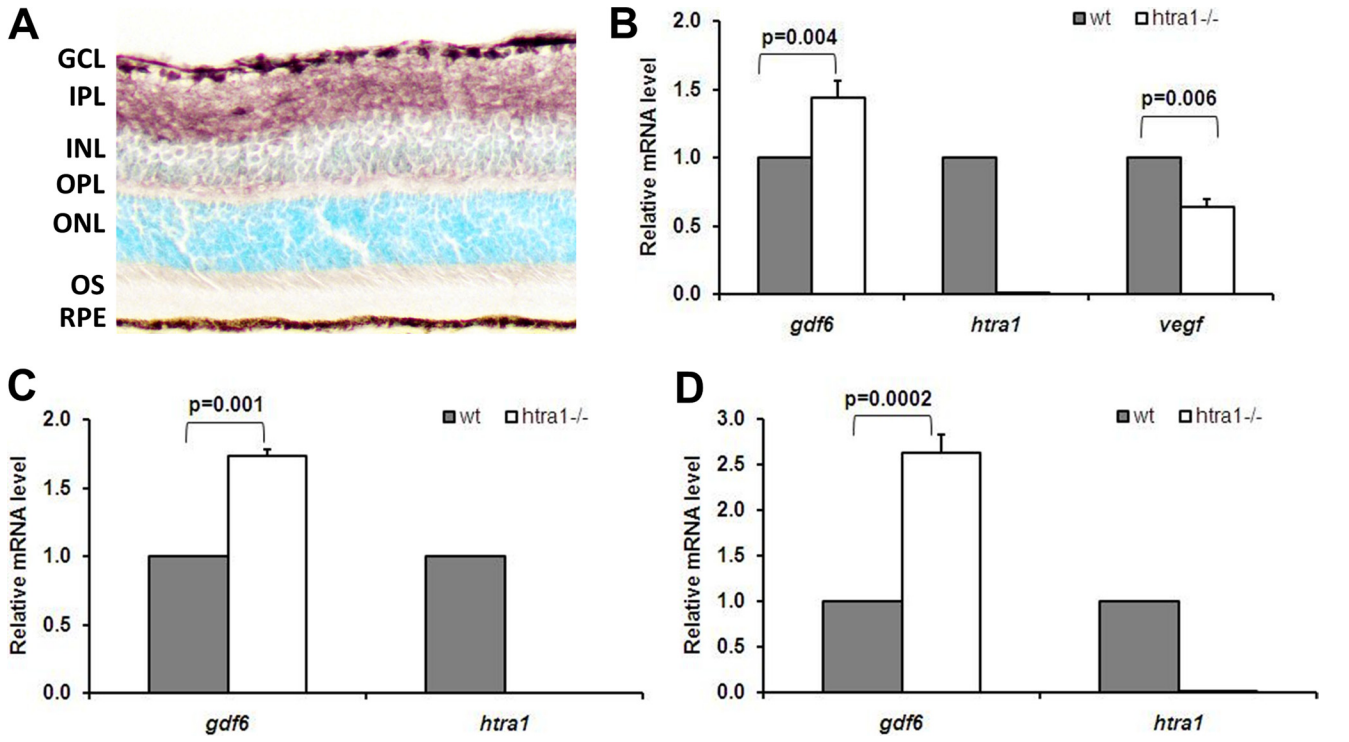

FIGURE 3. **Expression of *gdf6* and other AMD-related genes in mouse.** *A,* immunohistochemical staining of GDF6 in wild-type mouse retina. *GCL*, ganglion cell layer; *IPL*, inner plexiform layer; *INL*, inner nuclear layer; *OPL*, outer plexiform layer; *ONL*, outer nuclear layer; *OS*, outer segment. Quantitative-PCR analysis was performed for *gdf6*, *htra1*, and *vegf* in RPE layer (*B*), retinal tissue (*C*), and brain tissue (*D*) from the wild-type and *htra1*$^{-/-}$ mice. Relative mRNA levels were calculated by normalizing results with *gapdh* and presented as relative levels to wild-type tissue. *Error bars* represent S.E. $n = 6$ for wild-type and $n = 7$ for *htra1*$^{-/-}$ mice.

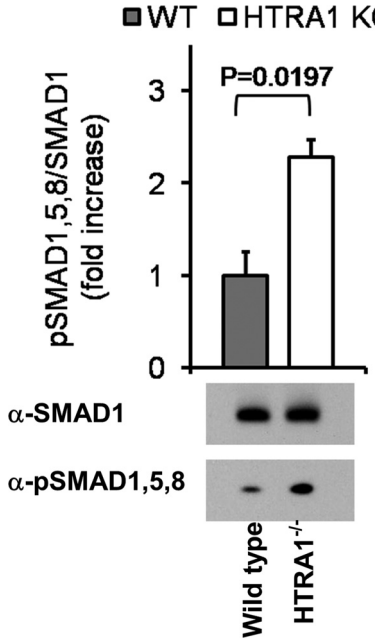

FIGURE 4. **Increased SMAD phosphorylation in brain tissue of *htra1*$^{-/-}$ mice.** A representative Western blot shows relative levels of SMAD1 and phosphorylated-SMAD1/5/8 signal in wild-type and *htra1*$^{-/-}$ mice. Mean ratios of the levels of phosphorylated SMAD1/5/8 (*pSMAD 1/5/8*) and SMAD1 were determined, and shown as fold-increase normalized against the ratio of the wild-type. *Error bars* represent S.E. $n = 3$ for wild-type and $n = 3$ for *htra1*$^{-/-}$ mice.

during normal growth of the brain and eye, whereas an elevated HTRA1 level contributes to increased and abnormal angiogenesis in the retina and therefore AMD phenotype (18). Consistent with this hypothesis, we observed a reciprocal gene expression regulation between HTRA1 and GDF6 in human lymphocytes as well as *htra1*$^{-/-}$ mice RPE and retina. In summary, our findings identify a novel disease gene *GDF6* for AMD and suggest a molecular basis for the angiogenesis pathway that links HTRA1 and TGF-β signaling through a negative regulation mechanism.

Acknowledgments—We thank members of Zhang laboratory for technical assistance and helpful discussions. We also thank Dr. Robert Graham for helpful discussions and sharing unpublished data.

REFERENCES

1. Friedman, D. S., O'Colmain, B. J., Muñoz, B., Tomany, S. C., McCarty, C., de Jong, P. T., Nemesure, B., Mitchell, P., and Kempen, J. (2004) *Arch. Ophthalmol.* **122,** 564–572
2. Haines, J. L., Schnetz-Boutaud, N., Schmidt, S., Scott, W. K., Agarwal, A., Postel, E. A., Olson, L., Kenealy, S. J., Hauser, M., Gilbert, J. R., and Pericak-Vance, M. A. (2006) *Invest. Ophthalmol. Vis. Sci.* **47,** 329–335
3. Churchill, A. J., Carter, J. G., Lovell, H. C., Ramsden, C., Turner, S. J., Yeung, A., Escardo, J., and Atan, D. (2006) *Hum. Mol. Genet.* **15,** 2955–2961
4. Grisanti, S., and Tatar, O. (2008) *Prog. Retin. Eye Res.* **27,** 372–390
5. Yang, Z., Tong, Z., Chen, Y., Zeng, J., Lu, F., Sun, X., Zhao, C., Wang, K., Davey, L., Chen, H., London, N., Muramatsu, D., Salasar, F., Carmona, R., Kasuga, D., Wang, X., Bedell, M., Dixie, M., Zhao, P., Yang, R., Gibbs, D., Liu, X., Li, Y., Li, C., Li, Y., Campochiaro, B., Constantine, R., Zack, D. J., Campochiaro, P., Fu, Y., Li, D. Y., Katsanis, N., and Zhang, K. (2010) *PLoS Genet.* **6,** e1000836
6. Tsuchiya, A., Yano, M., Tocharus, J., Kojima, H., Fukumoto, M., Kawaichi, M., and Oka, C. (2005) *Bone* **37,** 323–336
7. Grau, S., Richards, P. J., Kerr, B., Hughes, C., Caterson, B., Williams, A. S.,

Junker, U., Jones, S. A., Clausen, T., and Ehrmann, M. (2006) *J. Biol. Chem.* **281,** 6124–6129
8. Oka, C., Tsujimoto, R., Kajikawa, M., Koshiba-Takeuchi, K., Ina, J., Yano, M., Tsuchiya, A., Ueta, Y., Soma, A., Kanda, H., Matsumoto, M., and Kawaichi, M. (2004) *Development* **131,** 1041–1053
9. Launay, S., Maubert, E., Lebeurrier, N., Tennstaedt, A., Campioni, M., Docagne, F., Gabriel, C., Dauphinot, L., Potier, M. C., Ehrmann, M., Baldi, A., and Vivien, D. (2008) *Cell Death Differ.* **15,** 1408–1416
10. Hara, K., Shiga, A., Fukutake, T., Nozaki, H., Miyashita, A., Yokoseki, A., Kawata, H., Koyama, A., Arima, K., Takahashi, T., Ikeda, M., Shiota, H., Tamura, M., Shimoe, Y., Hirayama, M., Arisato, T., Yanagawa, S., Tanaka, A., Nakano, I., Ikeda, S., Yoshida, Y., Yamamoto, T., Ikeuchi, T., Kuwano, R., Nishizawa, M., Tsuji, S., and Onodera, O. (2009) *N. Engl. J. Med.* **360,** 1729–1739
11. Zumbrunn, J., and Trueb, B. (1996) *FEBS Lett.* **398,** 187–192
12. Mortlock, D. P., Guenther, C., and Kingsley, D. M. (2003) *Genome Res.* **13,** 2069–2081
13. Chang, C., and Hemmati-Brivanlou, A. (1999) *Development* **126,** 3347–3357
14. Asai-Coakwell, M., French, C. R., Berry, K. M., Ye, M., Koss, R., Somerville, M., Mueller, R., van Heyningen, V., Waskiewicz, A. J., and Lehmann, O. J. (2007) *Am. J. Hum. Genet.* **80,** 306–315
15. Hanel, M. L., and Hensey, C. (2006) *BMC Dev. Biol.* **6,** 43
16. Age-related Eye Disease Study (2001) *Arch. Ophthalmol.* **119,** 1439–1452
17. Yang, Z., Camp, N. J., Sun, H., Tong, Z., Gibbs, D., Cameron, D. J., Chen, H., Zhao, Y., Pearson, E., Li, X., Chien, J., Dewan, A., Harmon, J., Bernstein, P. S., Shridhar, V., Zabriskie, N. A., Hoh, J., Howes, K., and Zhang, K. (2006) *Science* **314,** 992–993
18. Jones, A., Kumar, S., Zhang, N., Tong, Z., Yang, J. H., Watt, C., Anderson, J., Amrita, Fillerup, H., McCloskey, M., Luo, L., Yang, Z., Ambati, B., Marc, R., Oka, C., Zhang, K., and Fu, Y. (2011) *Proc. Natl. Acad. Sci. U.S.A.* **108,** 14578–14583
19. Abramoff, M. D., Magalhaes, P. J., and Ram, S. J. (2004) *Biophoton. Int.* **11,** 36–42
20. Dewan, A., Liu, M., Hartman, S., Zhang, S. S., Liu, D. T., Zhao, C., Tam, P. O., Chan, W. M., Lam, D. S., Snyder, M., Barnstable, C., Pang, C. P., and Hoh, J. (2006) *Science* **314,** 989–992
21. Grau, S., Baldi, A., Bussani, R., Tian, X., Stefanescu, R., Przybylski, M., Richards, P., Jones, S. A., Shridhar, V., Clausen, T., and Ehrmann, M. (2005) *Proc. Natl. Acad. Sci. U.S.A.* **102,** 6021–6026
22. Grainger, D. J. (2004) *Arterioscler. Thromb. Vasc. Biol.* **24,** 399–404
23. Bakrania, P., Efthymiou, M., Klein, J. C., Salt, A., Bunyan, D. J., Wyatt, A., Ponting, C. P., Martin, A., Williams, S., Lindley, V., Gilmore, J., Restori, M., Robson, A. G., Neveu, M. M., Holder, G. E., Collin, J. R., Robinson, D. O., Farndon, P., Johansen-Berg, H., Gerrelli, D., and Ragge, N. K. (2008) *Am. J. Hum. Genet.* **82,** 304–319
24. Gonzalez-Rodriguez, J., Pelcastre, E. L., Tovilla-Canales, J. L., Garcia-Ortiz, J. E., Amato-Almanza, M., Villanueva-Mendoza, C., Espinosa-Mattar, Z., and Zenteno, J. C. (2010) *Br. J. Ophthalmol* **94,** 1100–1104
25. ten Dijke, P., and Arthur, H. M. (2007) *Nat. Rev. Mol. Cell Biol.* **8,** 857–869
26. Johnson, D. W., Berg, J. N., Baldwin, M. A., Gallione, C. J., Marondel, I., Yoon, S. J., Stenzel, T. T., Speer, M., Pericak-Vance, M. A., Diamond, A., Guttmacher, A. E., Jackson, C. E., Attisano, L., Kucherlapati, R., Porteous, M. E., and Marchuk, D. A. (1996) *Nat. Genet.* **13,** 189–195
27. Gallione, C. J., Repetto, G. M., Legius, E., Rustgi, A. K., Schelley, S. L., Tejpar, S., Mitchell, G., Drouin, E., Westermann, C. J., and Marchuk, D. A. (2004) *Lancet* **363,** 852–859
28. McAllister, K. A., Grogg, K. M., Johnson, D. W., Gallione, C. J., Baldwin, M. A., Jackson, C. E., Helmbold, E. A., Markel, D. S., McKinnon, W. C., Murrell, J., et al. (1994) *Nat. Genet.* **8,** 345–351
29. Neptune, E. R., Frischmeyer, P. A., Arking, D. E., Myers, L., Bunton, T. E., Gayraud, B., Ramirez, F., Sakai, L. Y., and Dietz, H. C. (2003) *Nat. Genet.* **33,** 407–411
30. Mazerbourg, S., Sangkuhl, K., Luo, C. W., Sudo, S., Klein, C., and Hsueh, A. J. (2005) *J. Biol. Chem.* **280,** 32122–32132